Rev. Adv. Mater. Sci. 52 (2017) 70-81

NANOMATERIALS BASED ON INTERMETALLIC (Co-Sn, Ni-Sn, Co-Ni) NANOPARTICLES STUDIED BY FTIR SPECTROSCOPY

I.N. Markova[1], I.Z. Zahariev[1], V.L. Milanova[1], D.I. Ivanova[1], M.B. Piskin[2], L.B. Fachikov[1] and E. Hristoforou[3]

[1]University of Chemical Technology and Metallurgy, 8, Kliment Ohridski blvd., 1756 Sofia, Bulgaria
[2]Yidiz Technical University, Davutpasa kampusu A 1003-1004 Esenler, Istanbul, Turkey
[3]National Technical University of Athens, 9 Herron Polytechniou Str., Zografou Campus, 15780, Athens, Greece

Received: June 21, 2017

Abstract. Intermetallic (Co-Sn, Ni-Sn, Co-Ni) nanoparticles have been synthesized through a wet chemical reduction with $NaBH_4$ in aqueous solutions of the chloride salts of Co, Ni, and Sn at room temperature. Also nanocomposite materials have been obtained in-situ using the same nanoparticles synthesis method but applying a template technique and using carbon-based support. The ratio of the metallic components has been chosen according to the phase diagrams of the relevant binary (Co-Sn, Ni-Sn, Co-Ni) systems: Co: Sn=35:65, Ni: Sn=45:55, Co: Ni=50:50. Graphite has been used as a support. To avoid the nanoparticle aggregation β-cyclodextrin has been added to the reaction solutions. The morphology, elemental and phase composition of the synthesized intermetallic nanocomposites have been investigated with SEM, EDS, and XRD respectively. The nanoparticles are different by shape and in size and exhibit a tendency to aggregate due to the unsaturated nanoparticle surface and the existing magnetic forces. The nanoparticle morphology is typical for an alloyed material. The formed phases are in accordance with the respective binary system phase diagrams: phases of CoSn and $CoSn_2$ for the Co-Sn (Co:Sn=35:65) nanoparticles, phases of Ni_3Sn_4, Ni_3Sn_2 and Ni_3Sn for the Ni-Sn nanoparticles (Ni: Sn=45:55), phases of Co and Ni for the Co-Ni nanoparticles (Co: Ni=50:50). The prepared nanopowders (Co-Sn, Ni-Sn, Co-Ni) and their carbon-containing nanocomposites have been studied by FTIR spectroscopy in the mid-IR region from 4000 to 400 cm^{-1}. On the basis of the collected FTIR spectra, respectively bands of absorption with peaks at the relevant frequencies the kind of vibrations (symmetric or asymmetric stretching and bending) of the created chemical bonds in different atom groups such as COH, CH_2, OH, H_2O, C=C, COOH, BO_3, BO_4, Me-O (Me=Co, Sn, Ni) have been determined.

1. INTRODUCTION

The synthesis of intermetallic nanoparticles and their nanocomposites is a priority area in materials science. This is a new approach in the technology of composite materials, which gives many opportunities to improve the existing characteristics, as well as to develop new properties. Challenge in the technology of the nanocomposites is the expansion of the variety of the nanoparticles used as a nanofiller, whereby new and specific properties of nanocomposites are expected.

In recent years, interest in nanosized particles increases due to their potential applications in key technology areas such as electronics, optics, chemical catalysis, biotechnology, and biomedicine. Synthesized are different metal, semiconductor and polymer nanoparticles, which are characterized by nonlinear optical and electronic properties of interest to different areas of science, engineering and technology [1-3].

Because of the small dimensions and the unsaturated surface state the nanoparticles tend to aggregate due to Van der Waals of interaction. This requires stabilization of the nanoparticles so that the forces of repulsion between the particles should balance the attraction between them. This can be achieved by chemically binding the particles with a

Corresponding author: I.N. Markova, e-mail: vania@uctm.edu

© 2017 Advanced Study Center Co. Ltd.

stabilizing agent, thereby creating a protective shell. This can control their size as well as their specific arrangement. The protective cover inactivates the surface to prevent the formation of agglomerates. It should be transparent, stable and susceptible to transformation. To stabilize the metal and semiconductor nanoparticles with protective shell polymer materials such as polyvinyl alcohol $(C_2H_4O)_x$, β-cyclodextrin ($C_{42}H_{70}O_{35}$) are used successfully . The latter represent hollow spheres which are implemented over wrap synthesized nanoparticles. By using IR spectroscopy with Fourier transform (FTIR) and X-ray diffraction (XRD) it has been proved that nanoparticles are formed on the walls of the hollow spheres [4-8].

In our previous work we reported for the synthesis of intermetallic Co-Sn, Ni-Sn, Co-Ni nanoparticles through a borohydride reduction in an aqueous solution of the corresponding chloride salts, as well as for a template synthesis using carbon-containing support [9-13]. As a result we got in situ nanocomposites with C-matrix and intermetallic nanoparticles that are suitable for electrodes in Li-ion batteries and magnetic materials for biomedical applications. We used β-cyclodextrin to avoid the aggregation of Co-Sn, Ni-Sn, Co-Ni nanoparticles during the template synthesis using graphite as a support. Having different elemental composition (Co-Sn, Ni-Sn, Co-Ni) the aim of the current work is to determine the nanoparticles morphology and phases formed by using SEM and XRD, as well as to study by FTIR spectroscopy the nanoparticles' surface state and nanointerface phenomena.

2. EXPERIMENTAL SET-UP

Intermetallic Co-Sn, Ni-Sn, and Co-Ni nanaoparticles are synthesized through a borohydride reduction method with 0.2 M $NaBH_4$ in a mixture of aqueous solutions of chloride salts of Co, Sn, and Ni (0.1 M $CoCl_2{\cdot}6H_2O$, 0.1 M $SnCl_2{\cdot}2H_2O$, 0.1 M $NiCl_2{\cdot}6H_2O$, respectively) at a ratio of metallic component chosen according to the phase diagram of the respective binary systems (Co:Sn=35:65, Ni:Sn=45:55, and Co:Ni=50:50). To reach the relevant ratio Co:Sn=35:65 we used 35 ml 0.1 M $CoCl_2{\cdot}6H_2O$ and 65 ml 0.1 M $SnCl_2{\cdot}2H_2O$, respectively for a ratio Ni:Sn=45:55 – 45 ml 0.1 M $NiCl_2{\cdot}6H_2O$ and 55 ml 0.1 M $SnCl_2{\cdot}2H_2O$ and for a ratio Co:Ni=50:50 - 50 ml $CîCl_2.6H_2O$ and 50 ml 0.1 M $NiCl_2{\cdot}6H_2O$. To fully complete the reduction process in the all cases the quantity of the reducing agent stabilized with NaOH is 100 ml 0.2 M $NaBH_4$. Citric acid ($C_6H_8O_7$) is used as a stabilizing ligand. In all cases we used quantity of 0.44 g/100 ml.

The synthesis is carried out in a double-wall cell ensuring a consecutively introducing of the initial solutions and continuously mechanical stirring of the reaction mixture with a magnetic stirrer. The experiments are run at room temperature and atmospheric pressure. The reduction process is completed in 2 minutes adding the reducing agent drop wise. Fine powder precipitates are obtained. They are filtrated, washed with a distillate water and ethanol and dried in a vacuum oven during 24 hours at 100 °C to prevent oxidation

Intermetallic Co-Sn, Ni-Sn, and Co-Ni nanocomposites are synthesized through the same borohydride reduction method using template technique and a carbon support at the same technological conditions as in the case of the synthesis without using a support (the same concentrations and quantities of the reaction solutions and reducing agent solution, the same ratio of the metallic components).

Fluorinated graphite (CF) and also graphite in a presence of β-cyclodextrin (β-CDx) are both used as a supports. As a result carbon-based nanocomposites are obtained in-situ. The used quantities of CF and β-CDx are respectively 0.36 g /100 ml. The ratio is 20% CF: 20% β-CDx: 60% intermetallic (Co-Sn, Ni-Sn, and Co-Ni) nanoparticles.

The morphology of the synthesized Co-Sn, Ni-Sn, and Co-Ni nanoparticles and their carbon-containing nanocomposites is investigated with of Scanning Electron Microscopy (SEM). The SEM images are made with a JEOL JSM 6390F (Japan) SEM microscope at accelerating voltage of 20 kV in a secondary electron regimes (SEI images are taken). The phase composition of the investigated samples is determined by X-ray diffraction (XRD). Powder X-raydiffraction data for phase identification were collected on a Philips PW 1050 automatic powder diffractometer using CuKα filtered radiation and Bragg- Brentanogeometry. Step-scan data were recorded in the angle interva 10–95° (2θ) with a step of 0.03°(2θ) and acounting time of 1 s. per step. Equal mass of powdered samples and identical sample holders were used in all measurements.

The intermetallic nanoparticles are also characterized by Infrared spectroscopy with Fourier transformation using a FTIR spectrophotometer EQUINOX 55 (Bruker) in mid- IR region of the spectrum – in the interval from 4000 to 400 cm^{-1}. FTIR spectra of the nanoparticles synthesized through a chemical reduction with $NaBH_4$ in a mixture of water solutions of the corresponding metal salts including using a support of graphite and also in the presence of β-cyclodextrin are taken.

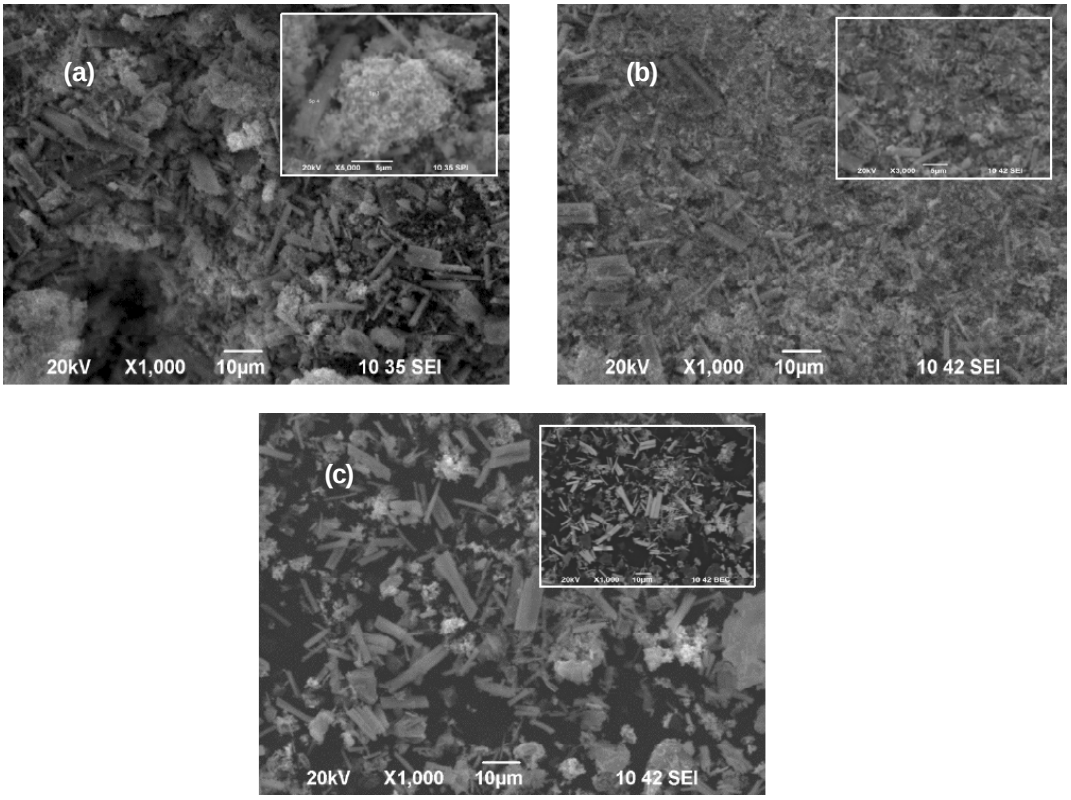

Fig. 1. SEM images at a magnification x 1000 in SEI regime: a-Co-Sn nanoparticles (Co: Sn=35:65) (sample 1), b-nanocomposites Co-Sn (Co: Sn=35:65)/CF (sample 2), c-nanocomposites Co-Sn (Co: Sn=35:65)/CF/β-cyclodextrin (sample 3).

3. RESULTS AND DISCUSSION

3.1. Investigation of Co-Sn nanoparticles obtained at a ratio Co: Sn=35:65 and their carbon-containing nanocomposites

3.1.1. Morphology of Co-Sn nanoparticles obtained at a ratio Co: Sn=35:65 and their carbon-containing nanocomposites. SEM results

Fig. 1a presents SEM images of Co-Sn nanoparticles synthesized at a ratio Co:Sn=35:65 (sample 1D), while in Figs. 1b and 1c SEM images of their carbon-containing nanocomposites based on graphite (sample 2D) and graphite in a presence of β-cyclodextrin (sample 3D) as a matrix are shown. The images are made at a magnification x1000 in SEI regime.

Generally, the SEM images of the Co-Sn nanoparticles show morphology typical for alloyed materials. The observed particles are irregular by shape and have form some aggregates. The bigger rectangular particles are most likely Sn based. It is observed that the graphite used as a support characterized by a flake like structure has influenced the nanoparticle formation during the template synthesis (Figs.1b and 1c). The nanoparticle morphology is of the graphite itself. Particles irregular by shape similar to the flake graphite particles are observed. The β-cyclodextrin added to the graphite prevents the nanoparticle aggregation (Fig. 1c).

3.1.2. Phase composition of Co-Sn nanoparticles obtained at a ratio Co: Sn=35:65 and their carbon-containing nanocomposites. XRD results

In Fig. 2 XRD patterns of the synthesized Co-Ni (Co: Ni=35:65) nanoparticles and their carbon-containing nanocomposites obtained through a template synthesis using graphite (CF) as a support and also graphite/β-cyclodextrin are presented.

The XRD spectra prove that during the synthesis of the Co-Sn nanoparticles at a ratio Co: Sn=35:65, including when carbon - containing supports are used two main phases of $CoSn_2$ and CoSn are formed. They are in accordance with the Co-Sn

binary system phase diagram. A phase of Sn is also observed. In the case of composites a phase of carbon is also present. The impure phase of SnO is probably due to oxidizing processes during the synthesis. According to literature data the $CoSn_2$ phase is a more suitable electrode material than the CoSn phase.

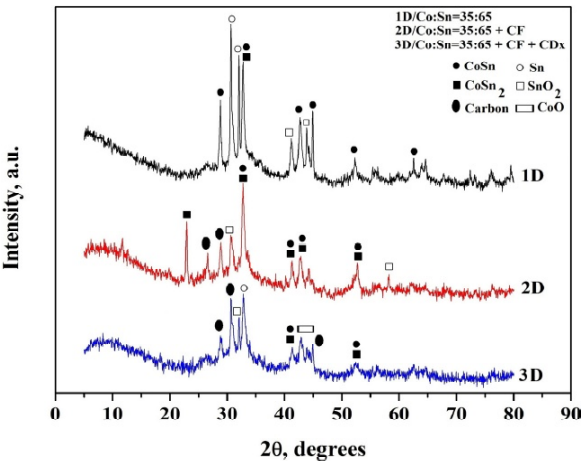

Fig. 2. XRD patterns Cî-Sn nanoparticles (Cî: Sn=35:65) and their carbon-containing nanocomposites: sample 1-Co-Sn nanoparticles, sample 2-nanocomposite Co-Sn/CF, sample 3-nanocomposite Co-Sn/CF/β-cyclodextrin.

3.1.3. FTIR spectra of Co-Sn nanoparticles obtained at a ratio Co: Sn=35:65 and their carbon-containing nanocomposites. FTIR spectroscopy results

Figs. 3a-3c demonstrate FTIR spectra of the Co-Ni (Co: Ni=35:65) nanoparticles (sample 1D) and their carbon-containing nanocomposites with matrix of graphite and also in the presence of β-cyclodextrin (sample 2D and sample 3D).

In Fig. 3a (FTIR spectrum of Co-Sn nanoparticles (Co:Sn=35:65) the bands of absorption in the frequency interval from 1400 to 500 cm^{-1} are due to vibrations of B-O bonds in BO_3 and BO_4 groups: the narrow and intensive band with a peak at 1365 cm^{-1} could be assigned to asymmetric stretching vibrations of B-O bonds in BO_3 groups, the very slight

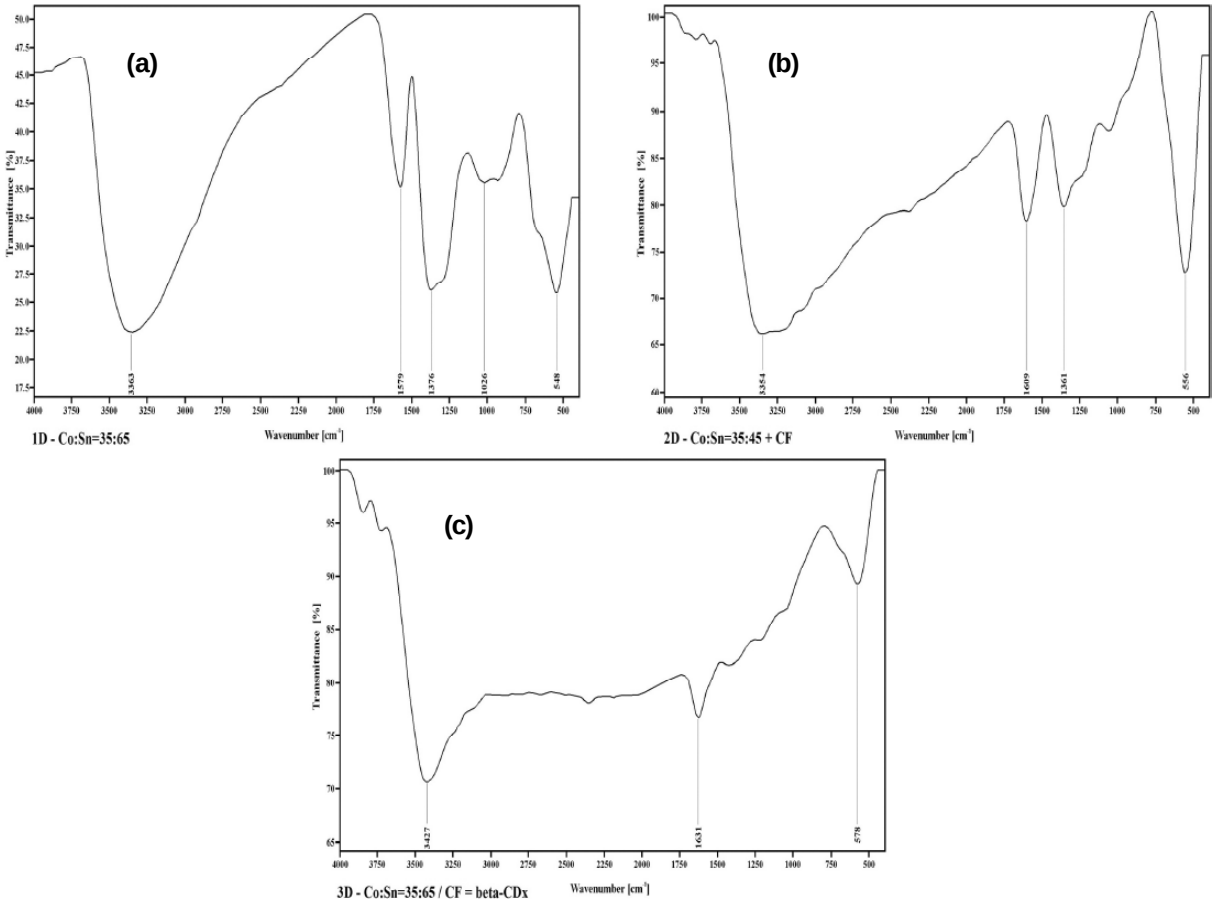

Fig. 3. FTIR spectra: a- sample 1/Co-Sn nanoparticles (Co: Sn=35:65), b-sample 2/ nanocomposites based on Co-Sn nanoparticles (Co: Sn=35:65) and graphite (CF) support, sample 3/nanocomposites based on Co-Sn nanoparticles (Co: Sn=35:65) and graphite (CF) as a support in a presence of β-CDx.

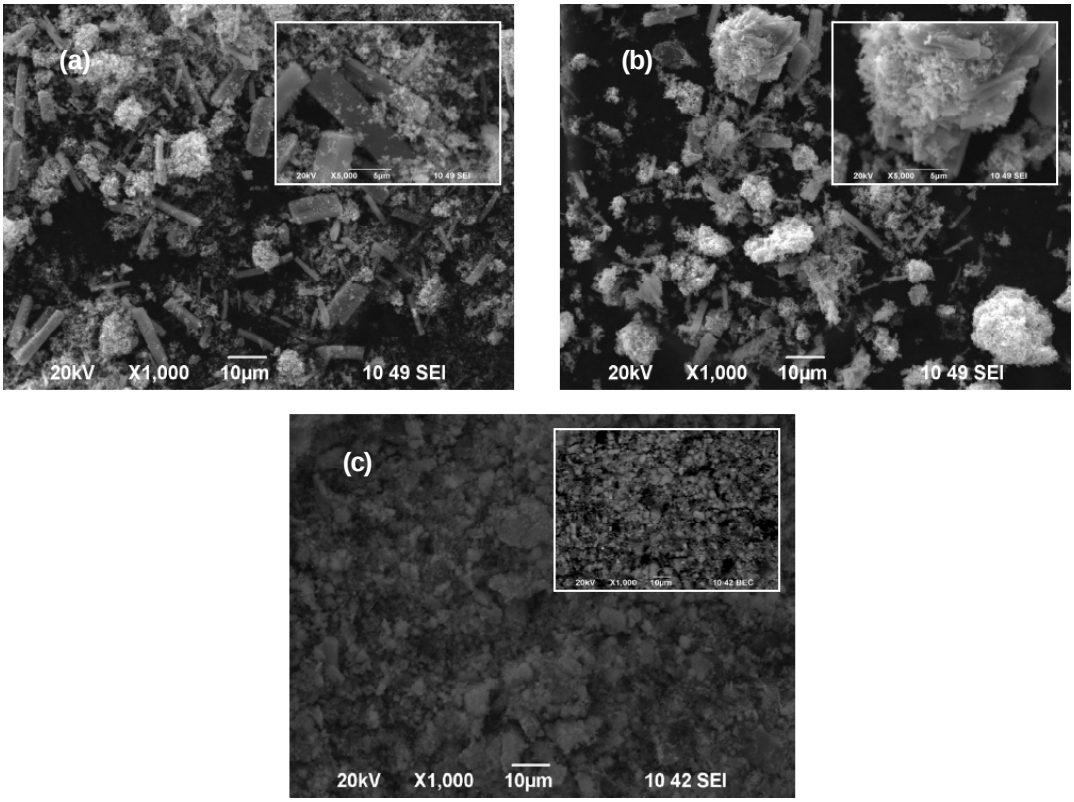

Fig. 4. SEM images at a magnification ×1000 in SEI regime: a-Ni-Sn nanoparticles/Co: Ni=45:55 (sample 4), b-nanocomposites Ni-Sn/CF (sample 5), c-nanocomposites Ni-Sn nanoparticles/CF+β-cyclodextrin (sample 6).

band with a peak at 1026 cm^{-1} is revealed to symmetric stretching vibrations of B-O bonds in BO_4 groups and the sharp band observed at 548 cm^{-1} is referred to bending vibrations of B-O bonds in BO_3 and BO_4 groups. The well expressed and intensive absorption band with a peak at 3365 cm^{-1} that can be seen in Fig. 3a is typical for stretching vibrations of O-H bonds in free OH groups, while the sharp band with a peak at 1579 cm^{-1} characterizes bending vibrations of H-O-H bonds in H_2O molecules adsorbed on the nanoparticle's surface. In the FTIR spectrum shown in Fig. 3b that belongs to composites of type Co-Sn nanoparticles/graphite (CF) bands with peaks at around the same frequencies are observed, but in the interval of 3400 - 700 cm^{-1} the bands are weaker and slighter expressed, while the band with a maximum at 556 cm^{-1} is stronger and sharper compared to that in the spectrum of the Co-Sn nanoparticles (Fig. 3). This band is a result from the overlap of the bands characterizing bending vibrations of B-O bonds in BO_3 and BO_4 groups and stretching vibrations of Co-O and Sn-O bonds in CoO and SnO oxides formed during the oxidation processes occurred through the reduction synthesis. Two FTIR spectra are distinguished by the shape and intensity of the bands in the interval from 1400 to 500 cm^{-1}. The very slight expressed bands in the interval of 3750-3600 cm^{-1} describe vibrations of C=C bonds due to the graphite used as a support for the template synthesis. The FTIR spectrum of the composites of type Co-Sn nanoparticles/graphite/β-cyclodextrin shown in Fig. 3c is disparate. Only three sharp and weak absorption bands with a maximum respectively at 3427 cm^{-1} and 1631 cm^{-1} (stretching and bending vibrations of O-H bonds, respectively) and 578 cm^{-1} (banding vibrations of B-O bonds) can be observed. Very slight vibrating signal at 1330 cm^{-1}, 1240 cm^{-1} and 1020 cm^{-1} that are probably related with B-O bond vibrations can be also detected. In the interval of 3600 – 3850 cm^{-1} the slight expressed bands could be assigned to vibrations of O-H bonds in hydroxyl-containing groups (CH_2OH) and C-O bonds in C-OH groups situated on the surface of the β-cyclodextrin, as well as they could be due to C=C bond vibrations in graphite support.

The FTIR spectra shown in Fig. 3 are different by both the shape and the intensity of the absorption band We can conclude that FTIR spectroscopy is a sensitive and suitable investigation method for studying nanomaterials because these differences can give qualitative information about the techno-

logical conditions of the reduction synthesis including the template synthesis with a carbon support.

3.2. Investigation of Ni-Sn nanoparticles obtained at a ratio Ni: Sn=45:55 and their carbon-containing nanocomposites

3.2.1. Morphology of Ni-Sn nanoparticles obtained at a ratio Ni: Sn=45:55 and their carbon-containing nanocomposites. SEM results

Fig. 4a present SEM images of Ni-Sn nanoparticles synthesized at a ratio Co:Sn=45:55 (sample 5D), while in Fig. 4b and Fig. 4c SEM images of their carbon-containing nanocomposites based on graphite (sample 6D) and in a presence of β-cyclodextrin (sample 7D) as a matrix are shown. The images are made at a magnification x1000 in SEI regime.

These images show the morphology of the Ni-Sn nanoparticles which are different in size. Small particles of 20-30 nm are observed. Bigger rectangular particles most probably from Sn can also be seen. When graphite is used as a support, the SEM images show flake like particles that are aggregated similar like the Co-Sn nanocomposites prepared at the same conditions. This is the morphology of the graphite itself. It can be seen in Fig. 4c that β-cyclodextrin added to the reaction solution prevents the nanoparticle's aggregation.

3.2.2. Phase composition of Ni-Sn nanoparticles obtained at a ratio Ni: Sn=45:55 and their carbon-containing nanocomposites. XRD Results

Fig. 5 presents XRD patterns of Ni-Sn nanoparticles and their graphite supported nanocomposites. In the all cases of Ni-Sn nanoparticles and their nanocomposites of type Ni-Sn nanoparticles/graphite including with β-cyclodextrin used as a capping agent the XRD analysis proves the formation of two main phases of Ni_3Sn_4 (2θ = 30°, 32°, 34°) and Ni_3Sn (2θ = 42°). Phase of graphite (2θ = 26°) is also present. Impurity phases of NiO (2θ = 26°, 62°) and SnO_2 (2θ = 32°) are also detected. Phase of Ni is presented too. According to the literature the obtained Ni_3Sn_4 phase is the best electrode material for Li-ion batteries. It means that the graphite (CF) is the better matrix for template obtaining the Ni-Sn alloy.

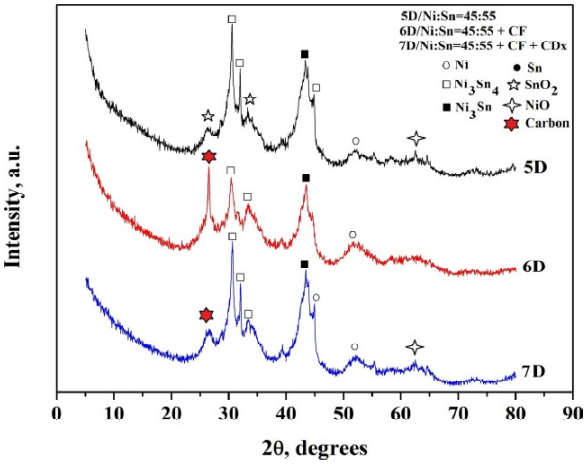

Fig. 5. XRD patterns: a-Ni-Sn (Ni: Sn=45:55) nanoparticles (sample 4), b-composite Ni-Sn nanoparticles (Ni:Sn = 45:55)/CF (sample 5), c-composite Ni-Sn nanoparticles (Ni:Sn = 45:55)/CF/ β-cyclodextrin (sample 6).

3.2.3. FTIR spectra of Ni-Sn nanoparticles obtained at a ratio Ni: Sn=45:55 and their carbon-containing nanocomposites. FTIR spectroscopy results

In Figs. 6a-6c FTIR spectra of Ni-Sn synthesized at a ratio Ni: Sn=45:55 (sample 5D) and their carbon-containing composites (sample 6D and sample 7D) are shown. The FTIR spectra of Ni-Sn nanoparticles synthesized using graphite as a support (sample 6D) and graphite in a presence of β-cyclodextrin (sample 7D) are similar by shape and position of the absorption bands to the spectra of Ni-Sn nanoparticles synthesized without using a support. Only intensity difference can be seen on the recorded bands in the investigated frequency interval. In the case of β–cyclodextrin the bands are wider and weaker expressed.

In the interval of 4000-3000 cm^{-1} the observed weak expressed bands describe stretching vibration of C=C bonds characteristic for graphite, C-H bonds in C-OH groups and C-H bonds in CH_2 groups typical for the citric acid used as a complexing agent. The band with a maximum at around 3440 cm^{-1} could be assigned not only to stretching vibrations of O-H bonds in OH groups, but also to bending vibrations of O-H bonds in hydroxyl-containing groups (CH_2OH) of β-cyclodextrin adsorbed on the nanoparticle surface. The bands in the interval of 1700-1000 cm^{-1} are due to stretching vibrations of C=C bonds belonging to the benzene ring of

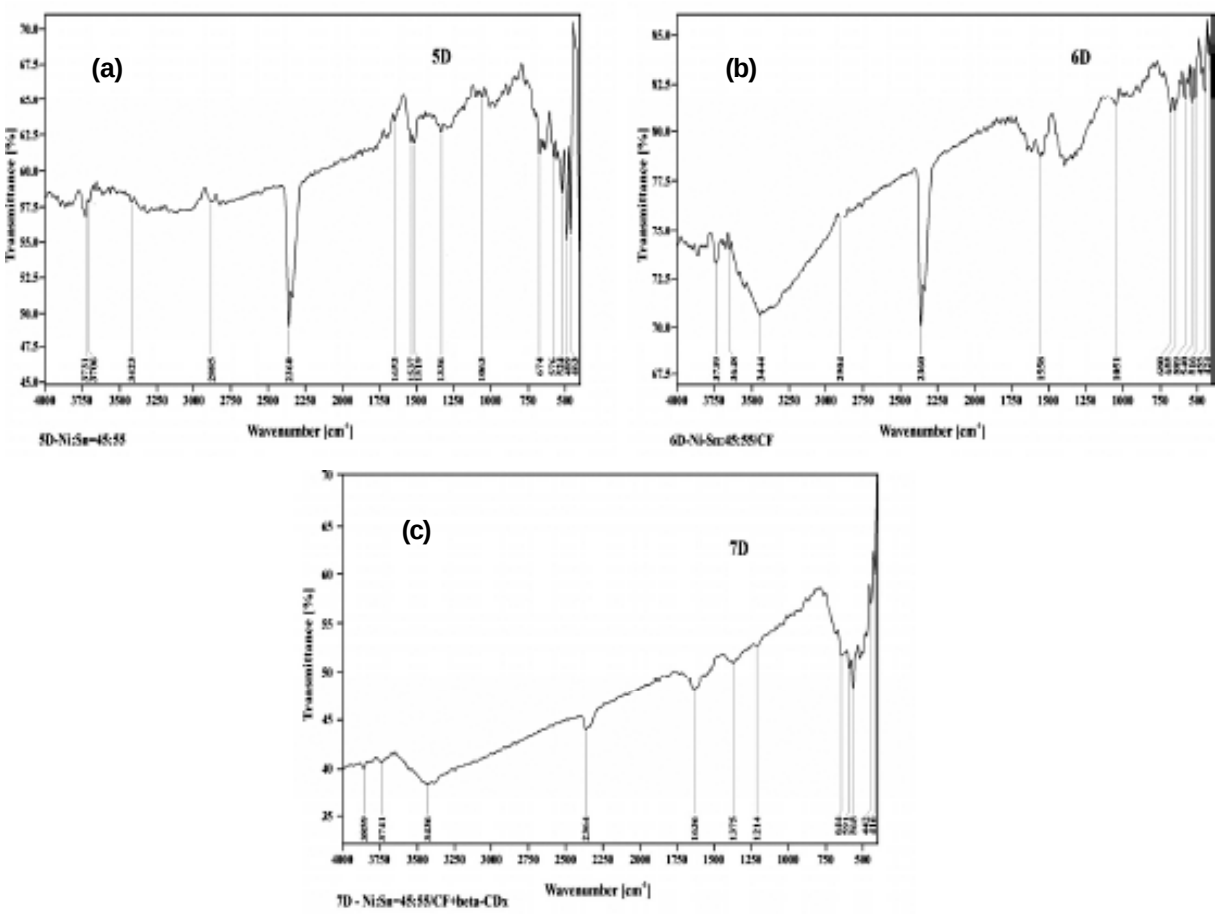

Fig. 6. FTIR spectra: a-Ni-Sn nanoparticles/Ni: Sn=45:55 (sample 4), b- nanocomposites based on Ni-Sn nanoparticles/Ni: Sn=45:55 and graphite (CF) support (sample 5), nanocomposites based on Ni-Sn nanoparticles/Ni:Sn=45:55 and graphite (CF) as a support in a presence of β- cyclodextrin (sample 6).

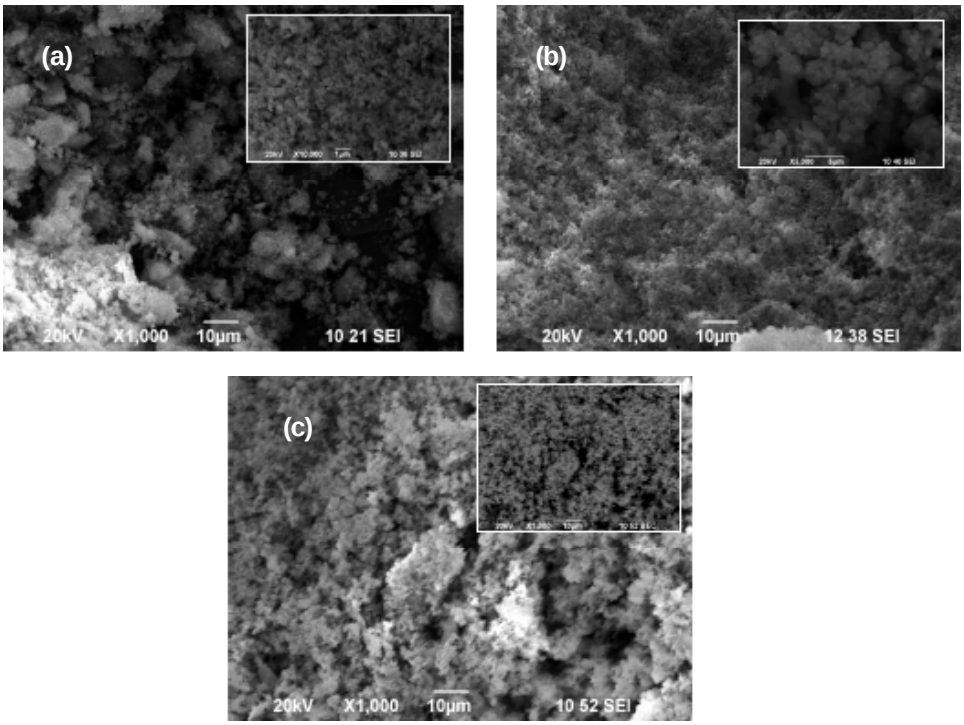

Fig. 7.SEM image at a magnification x1 000 in SEI regime: a-Co-Ni nanoparticles synthesized at a ratio Co:Ni=50:50 (sample 1=7), b-nanocomposites based on Co-Ni nanoparticles and graphite (CF) support (sample 8), c-nanocomposites based on Co-Ni nanoparticles and graphite (CF) support in a presence of β-cyclodextrin (sample 4=9).

β-cyclodextrin used during the nanoparticle synthesis. The bands in the interval of 1000–750 cm^{-1} are referred to symmetrical stretching vibrations of B-O bonds in BO_4 groups. The narrow and clear expressed bands in 600-400 cm^{-1} are related to bending vibrations of B-O bonds in BO_3 and BO_4 groups, but they could be assigned to bending vibrations of Ni-O and Sn-O bonds in the relevant NiO and SnO oxides. From here it could be inferred that the carbon-containing support like graphite and graphite/β-cyclodextrin doesn't change the shape of the FTIR spectra and the frequency at which the respective absorption bands characteritic vibrations of C-O, C-H, C=C, O-H, B-O, Ni-O, Sn-O bonds in the relevant atom groups have appeared.

3.3. Investigation of Co-Ni nanoparticles obtained at a ratio Co:Ni=50:50 and their carbon-containing nanocomposites

3.3.1. Morphology of Co-Ni nanoparticles obtained at a ratio Co: Ni=50:50 and their carbon-containing nanocomposites. SEM results

Fig. 7a presents SEM image of Co-Ni nanoparticles synthesized at a ratio Co:Ni=50:50 at a magnification x1000 in SEI regime, while in Figs. 7b and 7c SEM images of template synthesized Co-Ni nanoparticles using a support are shown, respectively graphite and graphite in the presence of β-cyclodextrin.

It's noticable that the support has influenced the nanoparticle's morphology. Very small nanoparticles are formed and tend to aggregate like in the case of Co-Sn and Ni-Sn nanoparticles. But in this case of Co-Ni nanoparticles the observed aggregates are almost the same in size and distributed homogeneously. This is probably due to the different elemental composition and formed phases. The morphology is typical for amorphous alloyed materials.

3.3.2. Phase composition Co-Ni nanoparticles obtained at a ratio Co: Ni=50:50 and their carbon-containing nanocomposites. XRD results

In Fig. 8 XRD patterns of Co-Ni nanoparticles synthesized at a ratio Co:Ni=50:50 and also the ones prepared by template technique using graphite as a support and in the presence of β-cyclodextrin are compared.

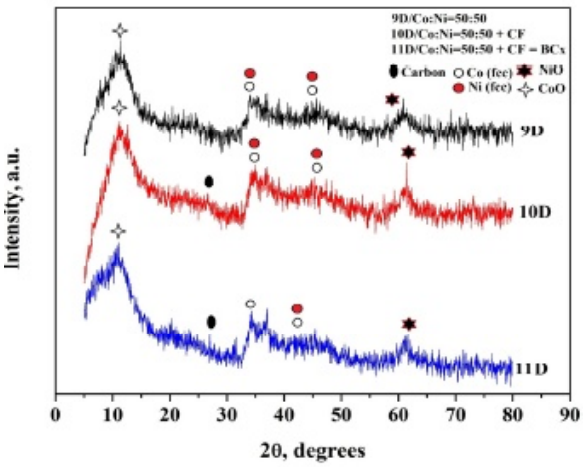

Fig. 8. XRD patterns of: a-Co-Ni nanoparticles synthesized at a ration Co: Ni=50:50 (sample 7), b-Co-Ni nanoparticles synthesized at a ratio Co: Ni=50:50 using graphite as a support (sample 8), c-Co-Ni nanoparticles synthesized at a ratio Co: Ni=50:50 using graphite as a support in the presence of β-cyclodextrin (sample 9).

The XRD patterns of Co-Ni nanoparticles and their carbon-containing nanocomposites show that during the synthesis of Co-Ni nanoparticles at a ratio of Co:Ni=50:50 and also when a carbon-based support is used two main face-cubic center phases of Co (fcc) and Ni(fcc) are formed that are in accordance with the phase diagram of the binary Co-Ni system. The peak at around 2θ value of 45° corresponds to both Co (fcc) and Ni (fcc) phases. The peak at 2θ value of 34° describes Co hexagonal centered phase (hcp). A phase of carbon is also detected at around 2θ2θ of value $2\theta \approx 26°$. The XRD analysis proves the formation of impurity of oxide phases of Co and Ni that are due to oxidizing processes. The peaks at around 2θ of values 12° and 37° are assigned respectively to CoO and Co_3O_4 phase. The peaks at around 2θ of value 62° are related to NiO phase.

3.3.3. FTIR spectra of Co-Ni nanoparticles obtained at a ratio Co: Ni=50:50 and their carbon-containing nanocomposites. FTIR spectroscopy results

The FTIR spectra of Co-Ni nanoparticles synthesized at a ratio Co:Ni=50:50 (sample 9D) and Co-Ni nanoparticles (Co:Ni=50:50) template synthesized

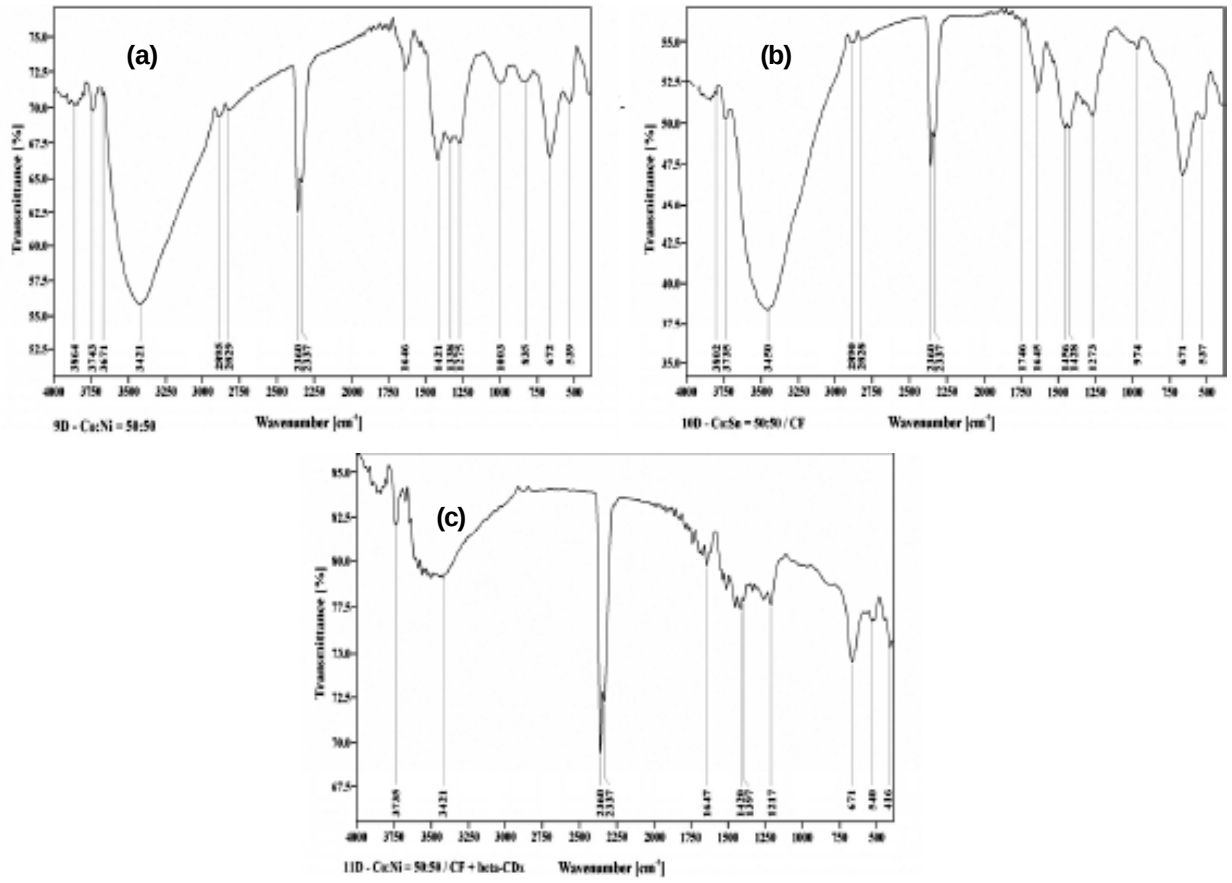

Fig. 9. FTIR spectra of: a-Co-Ni nanoparticles synthesized at a ratio Co:Ni=50:50 (sample 7), b-Co-Ni nanoparticles at Co:Ni=50:50 synthesized using fluorinated graphite as a support (sample 8), c-Co-Ni nanoparticles at Co:Ni=50:50 synthesized using fluorinated graphite as a support in the presence of β-cyclodextrin during the synthesis (sample 9), c-compared spectra of sample 7 and 9.

using graphite as a support (sample 10D) including using β-cyclodextrin during the synthesis (sample 11) are presented in Figs. 9a-9c. The experimental data on the basis of the collected FTIR spectra for the bands of absorption and the mode of the bond vibrations in the formed atom groups at the corresponding wavenumber (cm^{-1}) are given in Table 1.

It could be seen in Fig. 9b that the FTIR spectrum of Co-Ni nanoparticles (Co:Ni=50:50) using graphite as a support (sample 10D) seems similar to those of the sample 9D that presents Co-Ni nanoparticles synthesized at the same ratio Co:Ni=50:50 but without using a support during the synthesis (Fig. 9a), while the FTIR spectrum of Co-Ni nanoparticles synthesized using graphite in the presence of β-cyclodextrin during the synthesis distinguishes by the shape and intensity of the absorption bands (Fig. 9c). In the case of the sample 10D and 11D in the frequency region of 3900–3700 cm^{-1} slight expressed bands of absorption are observed: narrow and very slight absorption band at 3735 cm^{-1} could belong to stretching vibrations of C=C bonds resulting from the graphite used as a support during the synthesis and also to C-H bond vibrations in CH and CH_2 groups due to citric acid used as a complexing agent during the nanoparticle synthesis and β-cyclodextrin used as a capping agent to prevent the nanopartile's aggregation. In all cases the broad absorption bands with peaks respectively at 3421 cm^{-1} (Figs. 9a and 9c) and 3450 cm^{-1} (Fig. 9b) could be assigned to stretching vibrations of C-O bonds in C-OH groups and also to asymmetric stretching mode of vibrations v_1(OH) of O-H bonds in free OH groups. The slight expressed absorption bands with peaks at 2895 cm^{-1} and 2829 cm^{-1} (Fig. 9a), respectively at 2890 cm^{-1} and 2828 cm^{-1} (Figs. 9b and 9c) are due to stretching mode of vibrations of C-H bonds in CH_2 groups. These bands are probably overlapped by the band that is characteristic for the stretching vibrations of CH–OH bonds as a result from the used citric acid $C_6H_8O_7$.

The sharp and narrow bands of absorption with a maximum at 2360 cm^{-1} and 2337 cm^{-1} (Figs. 9a-

Table 1. Experimental data on the basis of the taken FTIR spectra for the mode of the bond vibrations in the formed atom groups at the corresponding wavenumber (cm^{-1}).

Experimental FTIR data for Co-Ni nanoparticles (Co:Ni-50:50) and their carbon-containing nanocomposites			
Absorption frequency, cm^{-1}	Chemical bond	Vibration mode	Atom group, molecule
3864, 38023743, 3735, 3671	C=CC-O	Stretching	GraphiteC-OH groups
3450	C-O	Stretching	C-OH groups
3450, 3421	O-H	Asymmetric stretching	Free OH groups
2895, 28902829, 2828	C-H	Stretching	CH_2 groups in $C_6H_8O_7$/citric acid
2360, 2337	O-HC-H	Asymmetric stretching	Free OH groups
		Stretching	CH_2 groups/citric acid
1746	C=C	Stretching	Graphite
1647, 1646, 1645	C-O	Stretching	COOH groups
1541	H-O-H	Bending	H_2O molecules
1456, 1428, 1421, 1420	C-H	Stretching	β-CDx
1338, 1275, 1273, 1217	B-O	Asymmetric stretching	BO_3 groups
1003	C-OB-O	Stretching	C-OH groups
		Symmetric stretching	BO_4 groups
974, 835	B-O	Bending	BO_4 groups
671, 672, 540, 539, 537	B-O	Bending	BO_3 and ByO_4 groups
416	Co-O, Ni-O	Stretching	Co_xO_y, Ni_xO_y

9c) could be refered to asymmetric stretching mode of vibrations v_1(OH) of O-H bonds in free OH groups and also to the stretching vibrations of C–H bonds due to the used of β-cyclodextrin during the synthesis. The detected sharp bands with a maximum respectively at about 1646 cm^{-1} (Fig. 9a), 1645 cm^{-1} (Fig. 9b), and 1647 cm^{-1} (Fig. 9c) characterize the vibrations of the C=O bond in the carboxyl group (COOH) of citric acid. These bands could be also due to bending mode of vibrations v_4(OH) of H-O-H bonds in H_2O molecules adsorbed on the nanoparticle surface. The band with a peak at 1746 cm^{-1} (Fig. 9b) has to belong to the stretching vibrations of the C=C bonds in the benzene ring of the β-cyclodextrin and in the graphite used as a support during the template synthesis.

In the case of sample 11D the very slight absorption band at 1397 cm^{-1} characterizing bending mode of vibrations δ(C-H) of C-H bonds in the primary and secondary hydroxyl groups of β-cyclodextrin is observed (Fig. 9c).The wide and very slight absorption band at 1003 cm^{-1} registered in Fig. 9a is due to stretching mode of vibrations *v*(C-O) of C-O bonds in the hydroxyl group citric acid.

According to the FTIR spectrum in Fig. 9 (frequency region of 1500–400 cm^{-1}) three modes of vibrations typical for B-O bonds in BO_3 and BO_4 groups forming different structural units are revealed as follows:

- asymmetric stretching mode of vibrations $v_3(BO_3)$ of B-O bonds in BO_3 groups in the frequency region of 1400 to 1200 cm^{-1} that are described by the bands with peaks at 1421 cm^{-1} 1338 cm^{-1} and 1275 cm^{-1} (Fig. 9a), 1456 cm^{-1} and 1428 cm^{-1} (Fig. 9b), and respectively at 1420 cm^{-1}, 1397 cm^{-1}, and 1217 cm^{-1} (Fig. 9c);
- symmetric stretching mode of vibrations $v_1(BO_4)$ of B-O bonds in BO_4 groups in the frequency region of 1000 to 850 cm^{-1} expressed by the bands with peaks at 1003 cm^{-1} and 835 cm^{-1} (Fig. 9a), 974 cm^{-1} (Fig. 9b)
- bending mode of vibrations $v_4(BO_3)$ and $v_4(BO_4)$ of B-O bonds in BO_3 and BO_4 groups in the frequency region of 800 to 400 cm^{-1} – bands with peaks at 672 cm^{-1} and 539 cm^{-1} (Fig. 9a), 671 cm^{-1} and 537 cm^{-1} (Fig. 9b), and respectively at 671 cm^{-1} and 540 cm^{-1} (Fig. 9c). The band at 416 cm^{-1} could be assigned to stretching vibrations of Me-O bonds in CoO and NiO, respectively(Fig. 9c).

The stretching vibrations at frequencies higher than 1000 cm^{-1} are characterized by brief and very strong B-O chemical bonds in the rigid BO_3 group, while the stretching vibrations at frequencies lower than 1000 cm^{-1} are typical for the weaker and longer chemical bonds in the BO_4 group. The BO_3 and BO_4 groups participate in the formation of pirobarate, dibarate, triborate, and tetraborate units (a structural units with a different number of BO_3 and BO_4

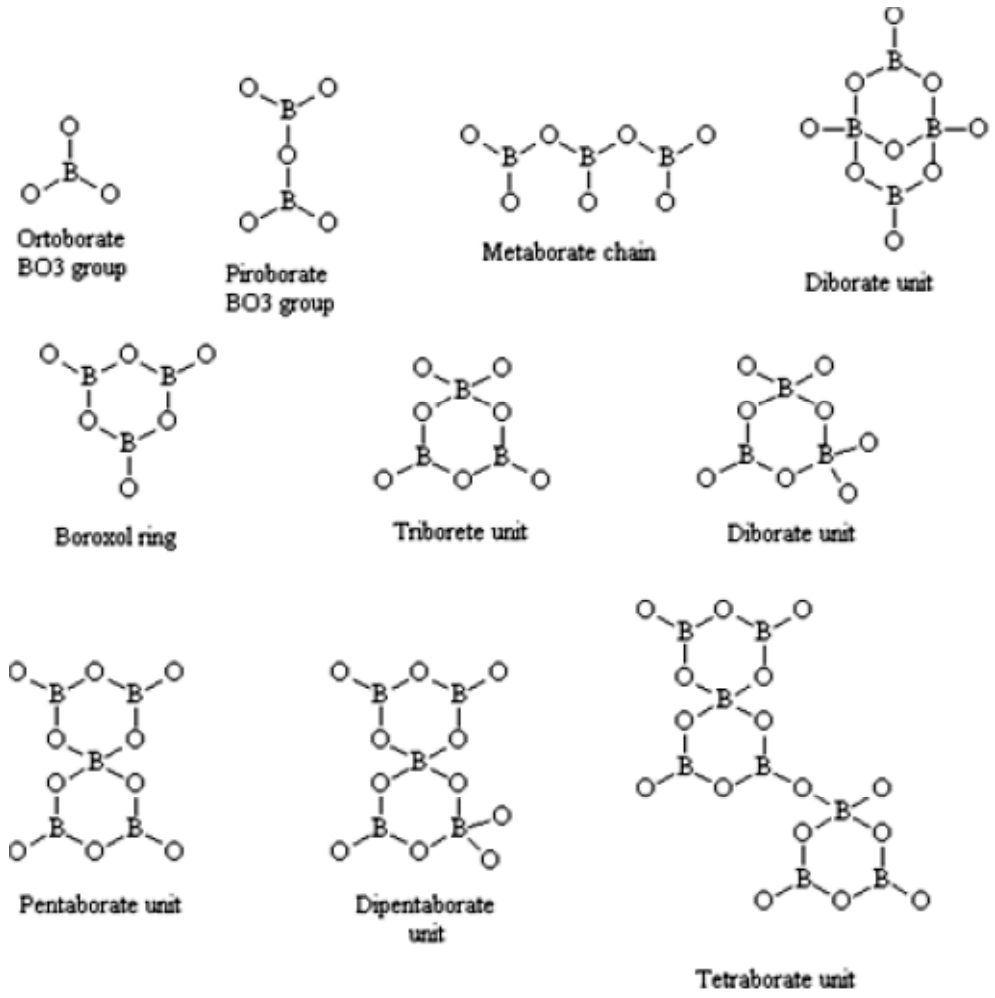

Fig. 10. Borate structural units.

groups) that are shown in Fig. 10. The FTIR spectroscopy study of the synthesized Co-Ni nanoparticles prove the creation of chemical bonds between boron and ogygen atoms, as well as the formation of BO_3 and BO_4 groups connected differently in boroxol rings $(B_3O_{4,5})_x$ and in boron structures formed from dibirate, triborate, and tetraborate units [14].

At the frequencies under 600 cm^{-1} sharp and slight expressed band of absorption can be seen (Fig. 9) corresponding to stretching vibrations of Me-O bonds: bands with peaks at 672 cm^{-1} (Fig. 9a) and 671 cm^{-1} (Figs. 9b and 9c) that characterize vibrations of Co-O bonds in CoO and Co_3O_4 oxides; bands with peaks at 539 cm^{-1} (Fig. 9a), 537 cm^{-1} (Fig. 9b) and respectively at 540 cm^{-1} and 417 cm^{-1} (Fig. 9c) that are typical for vibrations of Ni-O bonds in NiO oxides.

Generally, narrow sharp and slight expressed absorption bands under 600 cm^{-1} probably present overlapped absorption bands due to bending mode of vibrations of B-O bonds in BO_3 and BO_4 groups and respectively stretching mode of vibrations of metallic-oxygen bonds in metallic oxides (Co-O bonds in CoO, Co_3O_4, and Ni-O bonds in NiO).

In summary, basing on the FTIR study of the Co-Sn, Ni-Sn and Co-Ni nanoparticles synthesized through a borohydride reduction at a ratio metal/metal chosen according the phase diagrams of the relevant binary systems and also applying a template synthesis using a graphite as a support in the presence of β-cyclodextrin during the synthesis we can say that Infrared spectroscopy is a sensitive and suitable method for the investigation of the occurring nanoparticle surface phenomena. It is a reliable method in regards to identify the atom groups formed on the nanoparticle surface. FTIR spectra prove the creation of chemical bonds in atom groups on the nanosurface.

Infrared spectroscopy can distinguish the differences in the FTIR spectra due to synthesis conditions, including a different elemental composition, metal/metal ratio, and the use of a support for the nanoparticle template synthesis.

The position of the bands of absorption at the corresponding frequencies (wavenumber, cm^{-1}), the shape and intensity of the bands in the spectra give information about the mode of vibrations of the chemical bonds created between the relevant atoms in atom groups situated on the nanoparticle surface.

4. CONCLUSION

The performed wet brohydride reduction using a template synthesis with a carbon support (graphite) is an effective method and suitable down-up approach for in-situ preparation of new C-based nanocomposites with active intermetallic (Co-Sn, Ni-Sn, and Co-Ni) nanoparticles that are suitable for electrode and magnetic materials. Fine Co-Sn, Ni-Sn and Co-Ni alloy powders are obtained. The choice of a suitable matrix (graphite, including in the presence of β-cyclodextrin) and the optimization of the conditions for the Co-Sn, Ni-Sn, and Co-Ni alloy synthesis can bring to essential improvement of their properties. The obtained nanoparticles and their carbon-containing nanocomposites have morphology, which is typical for alloyed materials. The synthesized nanoparticles are about 100 nm in size and have an irregular shape. They tend to aggregate forming agglomerates of 0.5-100 μm in size. The supports used for the template synthesis influence the morphology and the structure of the obtained nanocomposites. The graphite support is appropriate in regards to nanoparticle dispersion. The mass ratio (Co, Ni):Sn and Co:Ni set in the synthesis of the intermetallic (Co-Sn, Ni-Sn, Co-Ni) nanoparticles controls the phase formation. The XRD analysis proves that stable phases of $CoSn_2$, Ni_3Sn_4 Co, Ni, which are in accordance with the Co-Sn, Ni-Sn, Co-Ni binary system phase diagrams can be achieved. The morphology, structure, elemental and phase composition of the prepared carbon-based nanocomposites with the synthesized intermetallic nanoparticles, respectively the formed stable microstructural phases are appropriate to be used as electrode nanocomposite materials instead of graphite in Li-ion batteries. Another potential application is in biomedicine as magnetic nanomaterials for biomedical applications as diagnostic tools and targeting treatment (drug delivery) in cancer and other diseases.

ACKNOWLEDGEMENTS

The authors acknowledge the financial support for this study provided by the National Science Fund at the Ministry of Education and Science – Bulgaria under the Contract DN 07/29–16.12.2016 (respectively under the Contract No 881/10.01.2017 of the Scientific Research Center at the UCTM-Sofia).

REFERENCES

[1] S. Schantz, H. T. Carlsson, T. Andersson, S. Erkselius, A. Larsson and O. Karlsson // *Langmuir* **23** (2007) 3590.

[2] D. J. Kim, S. M. Kang, B. Kong, W.-J. Kim, H.-J, Paik, H. Choi and I. S. Choi // *Macromol. Chem. Phys.* **206** (2005) 194.

[3] Y. Ding, Y. Hu, L. Zhang, Y. Chen and X. Jiang // *Biomolecules* **7** (2006) 1766.

[4] B. Cheng, Y. Zhu, W. Jiang, Z. Chen, C. Wang, G. Zhoi and P. Zhang // *Journal of Nanoparticles research* **1**, 4 (1999) 491.

[5] I. Markova-Deneva // *J. Univ. Chem. Technol. Metal.* **45** (2010) 351.

[6] N. V. Neamtu // *Journal of Nanomaterials and Biostructures* **6** (2011) 969.

[7] W. Lu, H. Yu, D. Sum and L. Lu // *J. Nanoengineering and Nanosystems* **228** (2014) 52.

[8] J. Huang, B. Zhang, Y. Y. Xie, W. W. K. Lye, Z.-L. Xu, S. Abouali, M. A.Garakani, J.-Q. Huang, T.-Yi Zhang, B. Huang and J.-K. Kim // *Carbon* **100** (2016) 329.

[9]. V. Milanova, T. Petrov, O. Chauvet and I. Markova *// Rev. Adv. Mater. Sci.* **37** (2014) 42.

[10] V. L. Milanova, M. B. Piskin, T.I. Petrov, T. E. Stankulov, I. D. Denev and I. N. Markova // *Rev. Adv. Mater. Sci.* **41** (2015) 52.

[11] V. Milanova, I. Markova**,** M. Piskin, T. Stankulov, T. Petrov and I. Denev // *J. Chem.Technol Metal* **50** (2015) 288.

[12] I. Z. Zahariev, E. Hristoforou and I. N. Markova // *J. Chem. Technol. Metal*. **50** (2017) 400.

[13] I. N. Markova, I. Z. Zahariev, M. T. Georgieva, D. Tzankov, D. I. Ivanova, M. B. Piskin and L. B. Fachikov // *Rev. Adv. Mater. Sci*. **50** (2017) 95.

[14] S. Ram and K. Ram // J*. Mater. Sci.* **23** (1989) 4541.